Journal of Thermal Analysis and Calorimetry, Vol. 64 (2001) 219–230

COMPARISON OF DIFFERENTLY BOUND MOLECULES IN THE GEL AND SUBGEL PHASES OF A PHOSPHOLIPID BILAYER SYSTEM

M. Kodama, H. Kato and H. Aoki

Department of Biochemistry, Okayama University of Science, 1-1 Ridai-cho Okayama 700-0005, Japan

Abstract

The thermal behavior associated with the melting of ice was investigated by differential scanning calorimetry (DSC) for the gel and *L*-subgel phases of dipalmitoylphosphatidylcholine (DPPC)–water system of varying water contents up to a full hydration. By calorimetric analysis previously developed by us, the numbers of differently bound water molecules were estimated, and used to construct water distribution diagrams (i.e., a plot of the cumulative numbers of these water molecules *vs.* water content) for the two phases. A comparison of the diagrams revealed the critical role of interlamellar water which changes from freezable to non-freezable one in a conversion of the gel to the *L*-subgel phase by the thermal annealing.

Keywords: DSC curve analysis, DPPC–water system, interlamellar water, subgel phase

Introduction

Phospholipids constitute the fundamental structure of a bilayer in biomembranes. Neutral phospholipids such as diacylphosphatidylcholine (PC) and diacylphosphatidylethanolamine (PE) occupy the majority of the total phospholipids in biomembranes, and exist in dispersions of multilamellar composed of their bilayers and water layers interposed between each other, when suspended in water. The lipid bilayers usually exist in either a gel or a liquid crystal phase depending on temperature. Thus, the gel phase, for which the hydrocarbon chains of the lipid molecule are in a solid-like state, transforms to the liquid crystal phase of liquid-like hydrocarbon chains at a certain temperature, generally called the T_m (gel-to-liquid crystal) transition temperature. Up to now, many studies on the stability of the gel phase have been performed for various phospholipids [1–15], and it has become apparent that the gel phase is metastable and converts to a more stable phase, generally called a subgel phase when the thermal annealing adopted for the gel phase is adequate. The subgel phase has been revealed to be present in two types, designated *L*- and *H*-subgel phases which transform to the gel and the liquid crystal phase on heating, respectively, i.e., these transitions appear, respectively, at temperatures lower and higher

1418–2874/2001/ $ 5.00
© 2001 Akadémiai Kiadó, Budapest
Akadémiai Kiadó, Budapest
Kluwer Academic Publishers, Dordrecht

than that of the T_m transition [4–7]. Previous studies of the subgel phase has been performed, mostly, focusing on lateral packings of the lipid molecules in an intrabilayer [7, 11–15]. Considering this, in our previous papers, the difference of the gel and *L*- and *H*-subgel phases in dimyristoylphosphatidylethanolamine (DMPE)–water system was investigated from a different point of view focusing on interlamellar water [4–6, 16]. Thus, in these studies, the numbers of interlamellar water molecules present in different bonding modes were estimated from the ice-melting curves of differential scanning calorimetry (DSC) and water distribution diagrams of varying water contents up to a full hydration were constructed for the gel and the two subgel phases. In the present study, the same calorimetric method was applied to dipalmitoylphosphatidylcholine (DPPC)–water system, and the numbers of differently bound water molecules for the gel phase were compared with those for the *L*-subgel phase which is present as the only subgel phase in this system.

Definitions and basic equations

Definitions of differently bound water molecules

Figure 1 shows the model of multilamellar structure of a phospholipid–water system. The water molecules in lipid–water systems are classified into three types; non-freezable interlamellar, freezable interlamellar, and bulk water. The structure of ice is characterized by networks of hydrogen bonds formed among neighboring water molecules. Therefore, water molecules that exists in regions between adjacent lipid head groups in an intrabilayer can be taken as non-freezable water. The reason for this is that the water molecules cannot participate in the formation of icelike hydrogen bonds, even when cooled extremely low temperatures, since they are confined within the narrow intrabilayer region. Also, water molecules that are tightly bound to lipid headgroups in an interbilayer region can be taken as non-freezable water. All these non-freezable water in lipid–water systems is found in regions between lamellae and so is designated non-freezable interlamellar water. The remainder of water molecules in the interbilayer region keeps the degree of freedom for their reorientations necessary to form icelike hydrogen bonds and so is designated freezable interlamellar water. The last is bulk water that exists outside bilayers, and on cooling it freezes in ice, the structure of which is very close to that of the most ordered hexagonal ice. However, the structure of ice derived from freezable interlamellar water is far different from that of hexagonal ice. Such a structural difference in the ice is reflected in its melting behavior observed by DSC. Thus, the ice derived from freezable interlamellar water begins to melt at temperatures as low as –40°C and continues melting up to about 0°C (broad ice-melting peak). In contrast, the ice derived from bulk water melts in a narrow temperature range around 0°C (sharp ice-melting peak).

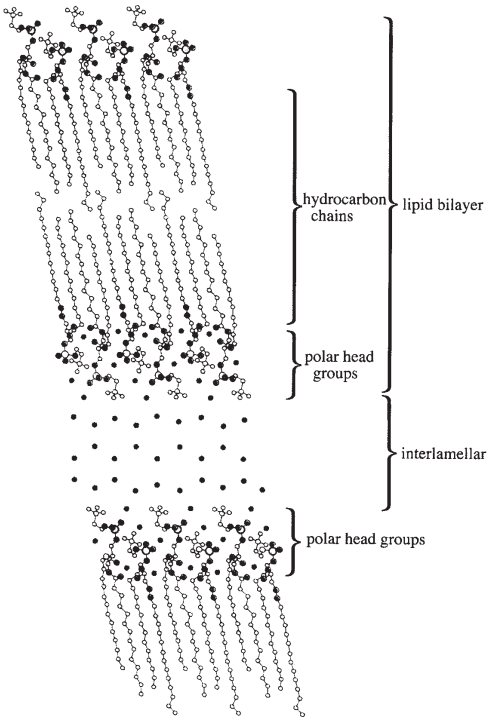

Fig. 1 A model structure of multilamellar bilayers of a diacylphospholipid–water system. A symbol of circles shows oxygen atoms for H_2O and lipid molecules

Equations and estimations for the number of water molecules

A correlation between the numbers of water molecules of these three types at a desired water content is given by the equation

$$N_T = N_{I(nf)} + N_{I(f)} + N_B \quad (1)$$

where N_T is the total number of water molecules per molecule of lipid and $N_{I(nf)}$, $N_{I(f)}$, and N_B are the numbers (per molecule of lipid) of non-freezable interlamellar, freezable interlamellar, and bulk water molecules, respectively. N_T is calculated from the amount of water added to a sample. When a molar mass is used, N_T is equal to the water/lipid molar ratio, N_w. By using the known value of melting enthalpy for hexagonal ice, 1.436 kcal (=6.01 kJ) per mole of water, Eq. (1) is replaced by

$$1.436\ (N_T - N_B) = 1.436\ (N_{I(nf)} + N_{I(f)}) \quad (2)$$

In Eq. (2), the first term, 1.436 N_T, represents the melting enthalpy, ΔH_T, for N_T moles of water added to 1 mole of lipid, assuming that the water is all present as bulk water, and so is a known value expressed in a unite of kcal (mol lipid)$^{-1}$. The second term, 1.436 N_B, corresponds to the melting enthalpy, ΔH_B, for N_B moles of water actu-

ally present as bulk water per mole of lipid and is experimentally determined from the ice-melting DSC curve. So, Eq. (2) is written as

$$\Delta H_T - \Delta H_B = 1.436\ (N_{I(nf)} + N_{I(f)}) \quad (3)$$

In the present study, for each water content of a lipid–water system, N_B was estimated from $\Delta H_B/1.436$ and subsequently the total number of interlamellar water molecules, N_I, which is equal to $N_{I(nf)}+N_{I(f)}$ in Eq. (3), was calculated from $(\Delta H_T - \Delta H_B)/1.436$.

Experimental techniques

Material and preparation of samples

1,2-Dipalmitoyl-*sn*-glycero-3-phosphatidylcholine (DPPC) used in the present study was purchased from Sigma Co. (St. Louis, MO).

The DPPC (approximately 30 mg) in a high pressure crucible cell (for a DSC apparatus) was dehydrated under a high vacuum (10^{-4} Pa) for at least 3 days and then the cell containing the dehydrated lipid was sealed off in a dry box filled with dry N_2 gas and weighed with a microbalance. In order to prepare a series of samples of varying water contents from 0 to at least 40 mass%, the desired amounts of water were added to the same dehydrated lipid, after each DSC. For each addition of water, the cell containing the lipid and the water was weighed with the microbalance. All the samples were annealed by repeating thermal cycling at temperatures above and below the T_m transition of the gel to the liquid crystal phase until the same transition behavior was observed. After this, the loss of water in the samples was checked with the microbalance, and the values of N_T (i.e, N_w) for the samples given by Eq. (1) were determined.

The samples of the gel phase were prepared by cooling the liquid crystal samples to temperatures below the T_m transition. On the other hand, the subgel samples were prepared by annealing the gel samples under adequate conditions related to a temperature range and a time period. Thus, a two-step annealing for the processes of nucleation and nuclear growth was applied [3]; the gel samples were kept at a temperature as low as –60°C for at least 6 h, after which thermal cycling was repeated between 0 to 4°C for periods of 1–3 weeks (depending on the water content of the samples).

DSC and deconvolution analysis

DSC was performed with a Mettler TA-4000 apparatus for the sample in the high pressure crucible cell (pressure resistant to 10 MPa) and on heating from –60°C to temperatures of the liquid crystal phase at a rate of 0.5°C min^{-1}. The DSC for the subgel samples obtained by annealing was initiated by cooling them to –60°C, but the DSC for the gel samples was performed by cooling the liquid crystal samples directly to –60°C.

ΔH_B in Eq. (3) is a chief determinant in the accuracy of this method because both N_B and N_I are estimated from its enthalpy, as discussed above. However, since

ice-melting DSC endotherms for bulk and freezable interlamellar water overlap at their basis, they were separated into individual components by a deconvolution analysis, in order to determine ΔH_B as accurately as possible. The deconvolution was performed according to a computer program for multiple Gaussian curve analysis [16].

Results and discussion

In Fig. 2, a series of typical DSC curves ranging in temperature from –50 to 70°C is compared for the gel and subgel samples of the DPPC–water mixture with increasing water content expressed in the water/lipid molar ratio (N_w). Furthermore, in Fig. 3, enlarged scale DSC curves of the two samples are compared at temperatures below 35°C. As revealed by comparing Fig. 2A with B, the gel samples lose a transition peak of the subgel to gel phases, which is observed only for the subgel samples, although the behavior of following two transition peaks of the gel ($L_{\beta'}$)-to-gel ($P_{\beta'}$) and gel($P_{\beta'}$)-to-liquid crystal phases (generally called the T_p and T_m transitions, respectively) is the same for the two samples [1–3, 8]. As is known, the subgel phase is present in two types, designated as *L*- and *H*-subgel phases, and the designations *L* and *H*

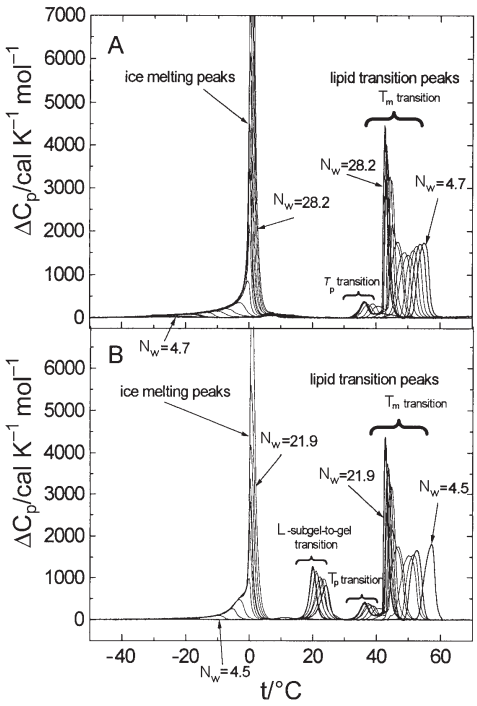

Fig. 2 Series of DSC curves for the gel (A) and *L*-subgel phases (B) of the DPPC–water system. Water contents expressed in the water/lipid molar ratio (N_w) range from 4.7 to 28.2 for the gel phase (A) and from 4.5 to 21.9 for the subgel phase (B), respectively. (1 cal=4.184 J)

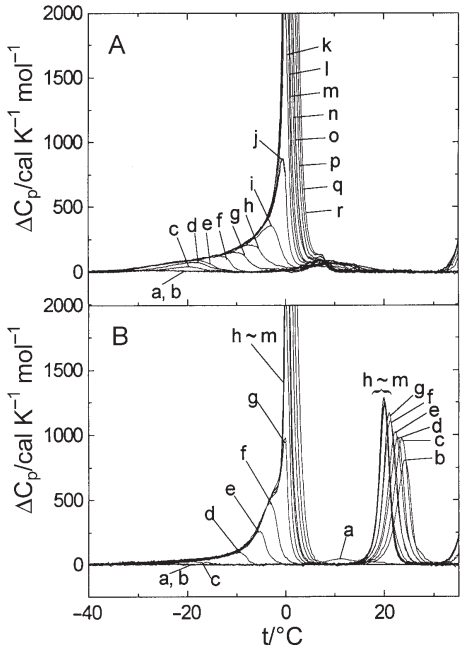

Fig. 3 Enlarged scale DSC curves at low temperatures for the gel (A) and *L*-subgel phases (B) of the DPPC–water system. N_w for the gel phase: a, 4.7; b, 5.3; c, 5.9; d, 6.0; e, 6.1; f, 6.7; g, 7.1; h, 7.8; i, 8.6; j, 10.2; k, 11.6; l, 12.9; m, 14.3; n, 16.6; o, 19.1; p, 21.9; q, 24.9; r, 28.2. N_w for the subgel phase: a, 4.5; b, 5.5; c, 6.0; d, 6.4; e, 7.8; f, 8.6; g, 10.2; h, 11.6; i, 12.8; j, 13.7; k, 15.9; l, 18.4; m, 21.9

for the subgel phases are due to their transition temperatures lower and higher than the T_m transition temperature, respectively [4–7]. Up to now, there is no report for the *H*-subgel phase of diacylPC–water systems. Presumably, this is because a large headgroup of the PC molecules prevents their much closer lateral packings required for the *H*-subgel phase, compared the *L*-subgel phase.

In Fig. 3, the difference in the ice-melting behavior between the gel and *L*-subgel phases is made clear. For the gel phase in Fig. 3A, the growth process of ice-melting peaks with increasing water content are as follows. The broad components of ice-melting peaks, derived from freezable interlamellar water, begin to appear at N_w~5 and grow in similar shapes (i.e., they cannot be superimposed on one another) up to at least N_w~8 where the sharp ice-melting peaks derived from bulk water appears at around 0°C. Above this, the sharp peaks continue to grow in superpositions. For the *L*-subgel phase shown in Fig. 3B, similar water content dependence of the ice-melting peaks is observed, but the broad ice-melting peaks of this phase are characterized by a shoulder at around –5°C and the onset temperature higher by 10°C than that (~ –40°C) of the corresponding peaks of the gel phase.

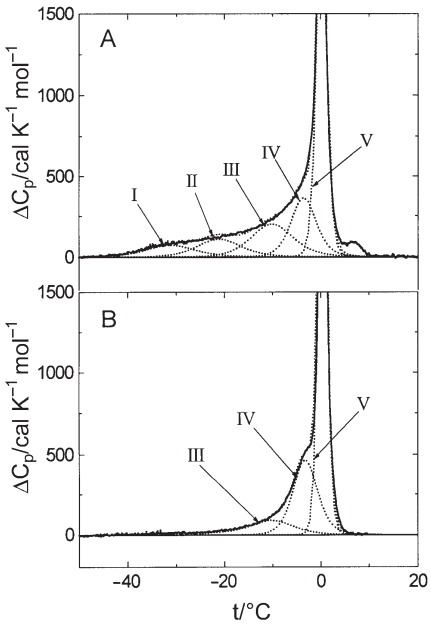

Fig. 4 Deconvoluted ice-melting curves for the gel (A) and *L*-subgel phases (B) of the DPPC–water system at the same water content (W_{H_2O}=28.0 mass%, N_w=15.9). The deconvoluted curves (I–V) and their sum (the theoretical curve) are shown by dotted lines and the DSC curves by solid lines

In Fig. 4, as an example, the results of the deconvoluted ice-melting curves are compared for the gel and *L*-subgel phases at the same water content of N_w=15.9. The present deconvolution was performed under the following conditions: (1) the theoretical curve given by the sum of individual deconvoluted curves is best fitted to the experimental DSC curve and (2) both the half-height width and the midpoint temperature of each deconvoluted curve are maintained almost constant throughout all the deconvolutions for varying water contents. For such a fully hydrated gel phase at N_w=15.9 (Fig. 4A), the broad ice-melting DSC peak for the freezable interlamellar water is deconvoluted into four curves of I, II, III, and IV. These deconvoluted curves appear in this order and become larger with increasing water content up to a full hydration at N_w~15. A deconvoluted curve V, comparable to the sharp ice-melting DSC peak for the bulk water, appears at N_w~8 and then continues to enlarge with increasing water content. For the *L*-subgel phase shown in Fig. 4B, the areas of both the deconvoluted curves I and II markedly decrease but that of the deconvoluted curve IV increases, compared with the corresponding deconvoluted curves for the gel phase shown in Fig. 4A.

The sum of the individual enthalpy changes of the deconvoluted curves I, II, III, and IV gives the ice-melting enthalpy (per mole of lipid) for the freezable interlamellar water, $\Delta H_{I(f)}$, and the enthalpy change of the deconvoluted curve V corre-

sponds to the ice-melting enthalpy (per mole of lipid) for the bulk water, ΔH_B, given in Eq. (3). In Fig. 5, the ice-melting enthalpies, $\Delta H_{I(f)}$ and ΔH_B, are plotted *vs.* N_w, respectively, together with ΔH_T given in Eq. (3). For the gel phase in Fig. 5A, the $\Delta H_{I(f)}$ curve intersects the abscissa at N_w~5, below which there is no freezable water (i.e., only non-freezable interlamellar water exists). So, the value of N_w=5 could give the maximum number of non-freezable interlamellar water molecules, by assuming limited uptake of this water within a limited space of the intrabilayer regions. So, the limiting, maximum number of non-freezable interlamellar water molecules for the gel phase of the DPPC system is $5H_2O$ per mole of lipid. On the other hand, the ΔH_B curve for the gel phase increases linearly and parallel to the theoretical ΔH_T line at water contents above N_w~15, indicating that ΔH_T–ΔH_B in Eq. (3) becomes the same at all water contents above the boundary N_w (~15). Such a parallel ΔH_B curve proves limited uptake of the interlamellar water (i.e., limited hydration of the lipid bilayers), so that a fully hydrated gel phase of the DPPC system is attained at the boundary N_w. For the limited hydration, the limiting, maximum number of total (non-freezable plus freezable) interlamellar water molecules can be also determined graphically by ex-

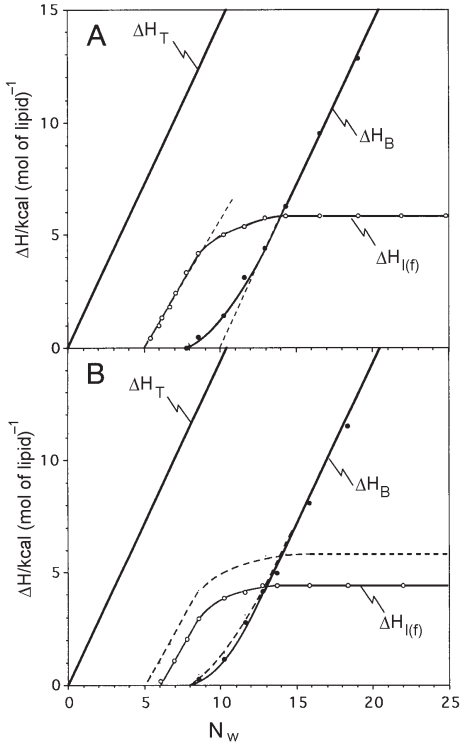

Fig. 5 Plots of the ice-melting enthalpies, ΔH_T, ΔH_B, and $\Delta H_{I(f)}$, *vs.* N_w for the gel (A) and *L*-subgel phases (B) of the DPPC–water system. Dashed lines in B present the ΔH_B and $\Delta H_{I(f)}$ curves shown for the gel phase in A, respectively

trapolating the linear ΔH_B curve to non-linear regions (dashed lines) below N_w~15. Thus, N_w of the intersection point just corresponds to the maximum number of interlamellar water molecules, i.e., $10H_2O$ per mole of lipid for the gel phase of the DPPC system. As a result, the number of freezable interlamellar water molecules for the fully hydrated gel phase is estimated to be 5 (=10– 5)H_2O per molecule of lipid, corresponding to the maximum number of this water molecules for the gel phase.

For the *L*-subgel phase in Fig. 5B, the $\Delta H_{I(f)}$ curve is lower than that for the gel phase (dashed lines) over all water contents tested, and its extrapolated line intersects the abscissa at N_w~6, giving the maximum number of non-freezable interlamellar water molecules, $6H_2O$ per mole of lipid, which is larger by $1H_2O$/lipid than the corresponding value ($5H_2O$/lipid) for the gel phase. However, the ΔH_B curve for the subgel phase is almost consistent with that for the gel phase (dashed lines), indicating nearly the same number of bulk water molecules (N_B) for the two phases of the same water content and so the number of total interlamellar water molecules, N_I ($=N_{I(nf)}+N_{I(f)}$), given by $N_T–N_B$ becomes nearly equal between the two phases of the same water content. However, Fig. 5B reveals that $N_{I(f)}$ at the same water content is larger for the gel phase than for the subgel phase and

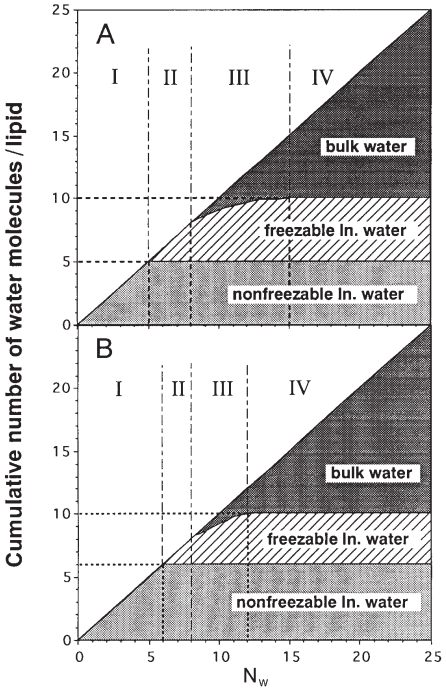

Fig. 6 Water distribution diagrams for the gel (A) and *L*-subgel phases (B) of the DPPC–water system. The cumulative numbers of water molecules (per mole of lipid) present as non-freezable and freezable interlamellar water and as bulk water are plotted *vs.* N_w. The designations I, II, III and IV represent four water content regions where the individual numbers of these differently bound water molecules were estimated according to Table 1

contrary to this, as discussed above, $N_{I(nf)}$ in the maximum value is greater by $1H_2O$/lipid for the subgel phase than for the gel phase. Thus, N_B, N_I, $N_{I(f)}$ and $N_{I(nf)}$ for the gel and *L*-subgel phases at the same water content of the DPPC system are as follows: Similarly to N_B, $N_{I(f)}$ for the gel phase is nearly equal to that for the subgel phase; $N_{I(f)}$ is subgel phase < gel phase; and $N_{I(nf)}$ is gel phase<subgel phase. These results indicate that in the conversion of the gel to *L*-subgel phases, a structural change of water molecules occurs within the interlamellar water, independently of the bulk water, and the interlamellar water changes from freezable to non-freezable one up to one molecule of H_2O per mole of lipid at a maximum. Accordingly, the freezable interlamellar water present in the gel phase reveals a requirement for the appearance of the *L*-subgel phase of the DPPC system. In fact, as shown in Fig. 2B (a), no endotherm due to the gel-to-subgel phase transition is observed for $N_w<5$ where the gel phase is free from the freezable interlamellar water (Fig. 6A). The similar structural change in the interlamellar water has been previously reported by us for the conversion of the gel to *L*-subgel phases of dimyristoylphosphatidylethanolamine (DMPE)–water system [5]. Presumably, the extra non-freezable interlamellar water, which arises from the freezable interlamellar water in the gel phase, is needed to realize lateral packings of lipid molecules required for the *L*-subgel phase. On the other hand, for the *H*-subgel phase of the DMPE–water system, almost no interlamellar water has been also reported by us [6].

Table 1 A summary in estimations of the numbers of non-freezable interlamellar, freezable interlamellar, and bulk water molecules, $N_{I(nf)}$, $N_{I(f)}$, and N_B, respectively, per lipid molecule for the gel (A) and *L*-subgel phases (B) of the DPPC–water system in four water content regions I, II, III and IV shown in Fig. 6

		Number of water molecules/per mol of lipid		
	N_w	$N_{I(nf)}$	$N_{I(f)}$	N_B
(A): Gel phase				
I	$N_w<5$	N_T[a]	0	0
II	$5\leq N_w<8$	5	(N_T-5)	0
III	$8\leq N_w<15$	5	$(\Delta H_T$[b]$-\Delta H_B$[c]$)/1.436-5$	$\Delta H_B/1.436$
IV	$N_w\geq 15$	5	5	$\Delta H_B/1.436$
(B): *L*-subgel phase				
I	$N_w<6$	N_T[a]	0	0
II	$6\leq N_w<8$	6	(N_T-6)	0
III	$8\leq N_w<12$	6	$(\Delta H_T$[b]$-\Delta H_B$[c]$)/1.436-6$	$\Delta H_B/1.436$
IV	$N_w\geq 12$	6	4	$\Delta H_B/1.436$

[a] N_T is the total number of water molecules per molecule of lipid add to the sample and is equal to N_w
[b] ΔH_T is equal to 1.436 N_w ($=N_T$)
[c] ΔH_B is the ice-melting enthalpy per mole of lipid for bulk water
All the numbers of water molecules (per mole of lipid) have a standard deviation of $\pm 0.2H_2O$/lipid which comes from the deconvolution analysis used in the present study.

Figures 6A and B compare water distribution diagrams (i.e., plots of the cumulative numbers of water molecules, $N_{I(nf)}+N_{I(f)}+N_B$, per mole of lipid *vs.* N_w) for the gel and *L*-subgel phases of the DPPC system. Details of the estimations of $N_{I(nf)}$, $N_{I(f)}$, and N_B in four water content regions (I, II, III, and IV) shown in Fig. 6 are summarized in Table 1. The main difference between Figs 6A and B is a greater amount of the non-freezable interlamellar water for the subgel than for the gel phase observed for $N_w \geq 5$ (i.e., the lower limit of water content for the appearance of the *L*-subgel phase) and the limiting, maximum difference in the amount of this water, $1H_2O$/lipid, is observed for $N_w > 6$. Another point to note is the existence of a special region [16–21], previously designated as a pre-region, where the bulk water appears although the limiting, maximum amount of interlamellar water is not yet reached. The similar pre-region has been reported by us for DMPE–water [16] and diacylphosphatidylglycerol (PG)–water systems [20, 21]. The pre-regions for the gel and *L*-subgel phases of the present system are located in the water content region III in Figs 6A and B, respectively, where the amounts of the freezable interlamellar water increase gently up to the limiting, maximum values of 5(=10–5) H_2O/lipid and 4(=10–6) H_2O/lipid for the gel and *L*-subgel phases, respectively. In this connection, in Fig. 5, non-linear increases of both the ΔH_B and $\Delta H_{I(f)}$ curves in the pre-region are observed for both the gel (A) and the *L*-subgel phase (B).

References

1 M. J. Ruocco and G. Shipley, Biochim. Biophys. Acta, 691 (1982) 309.
2 M. Kodama, Thermochim. Acta, 109 (1986) 81.
3 M. Kodama, H. Hashigami and S. Seki, J. Colloid Interface Sci., 117 (1987) 497.
4 M. Kodama, H. Inoue and Y. Tsuchida, Thermochim. Acta, 266 (1995) 373.
5 H. Aoki and M. Kodama, J. Thermal Anal., 49 (1997) 839.
6 M. Kodama, H. Kato and H. Aoki, Thermochim. Acta, 352 (2000) 213.
7 M. Kodama, H. Aoki and T. Miyata, Biophys. Chem., 79 (1999) 205.
8 S. C. Chen, J. M. Sturtevent and B. J. Gaffeny, Proc. Natl. Acad. Sci. USA, 77 (1980) 5060.
9 H. H. Mantsch, S. C. Hsi, K. W. Butler and D. G. Cameron, Biochim. Biophys. Acta, 728 (1983) 325.
10 S. Mulukutla and G. G. Shipley, Biochemistry, 23 (1984) 2514.
11 D. A. Wilkinson and J. F. Nagle, Biochemistry, 23 (1984) 1538.
12 D. A. Wilkinson and T. J. McIntosh, Biochemistry, 25 (1986) 295.
13 R. M. Epand, B. Gabel, R. F. Epand, A. Sen, S. W. Hui, A. Muga and W. K. Surewicz, Biophys. J., 63 (1992) 327.
14 P. Laggner, K. Lohner, G. Degovics, K. Muller and A. Schuster, Chem. Phys. Lipids, 44 (1987) 31.
15 R. D. Koynova, B. G. Tenchov, P. J. Quinn and P. Laggner, Chem. Phys. Lipids, 48 (1988) 205.
16 M. Kodama, H. Aoki, H. Takahashi and I. Hatta, Biochim. Biophys. Acta, 1329 (1997) 61.
17 G. Klose, B. König, H. W. Meyer, G. Schulze and G. Degovics, Chem. Phys. Lipids, 47 (1988) 225.

18 J. F. Nagle, R. Zhang, T. Stephanie-Nagle, W. Sun, H. I. Petrache and R. M. Suter, Biophys. J., 70 (1996) 1419.
19 K. Gawrisch, W. Richter, W. A. Möps, P. Balgavy, K. Arnold and G. Klose, Studia Biophys., 108 (1985) 5.
20 M. Kodama, J. Nakamura, T. Miyata and H. Aoki, J. Thermal Anal., 51 (1998) 91.
21 H. Aoki and M. Kodama, Thermochim. Acta, 308 (1998) 77.